

The Riemann zeros and the cyclic Renormalization Group

Germán Sierra

Instituto de Física Teórica, CSIC-UAM, Madrid, Spain

(Dated: October 2005)

Abstract

We propose a consistent quantization of the Berry-Keating Hamiltonian xp , which is currently discussed in connection with the non trivial zeros of the Riemann zeta function. The smooth part of the Riemann counting formula of the zeros is reproduced exactly. The zeros appear, not as eigenstates, but as missing states in the spectrum, in agreement with Connes adelic approach to the Riemann hypothesis. The model is exactly solvable and renormalizable, with a cyclic Renormalization Group. These results are obtained by mapping the Berry-Keating model into the Russian doll model of superconductivity. Finally, we propose a generalization of these models in an attempt to explain the oscillatory part of the Riemann's formula.

PACS numbers: 02.10.De, 05.45.Mt, 11.10.Hi

arXiv:math/0510572v2 [math.NT] 3 Nov 2005

I. INTRODUCTION

The Riemann hypothesis (RH) is a central problem in Pure Mathematics due to its connection with Number theory and other branches of Mathematics and Physics. The RH is the statement that all the non trivial zeros of the zeta function $\zeta(s)$ lie on the critical line $Re(s) = 1/2$ [1]. Most of the physical approaches to prove the RH are inspired by the old Polya and Hilbert conjecture, which states that the imaginary part, E_a , of the Riemann zeros $\zeta(\frac{1}{2} + iE_a) = 0$, are the eigenvalues of a Hamiltonian and thus real numbers if the RH is true [2]. This approach is supported by the statistical properties of the zeros, the Montgomery-Odlyzko law [3, 4], based on the Gaussian Unitary Ensemble distribution (GUE) [5], and also by the quantum chaos interpretation of the oscillatory part of the Riemann counting formula of the zeros [6]. Berry has proposed that the Riemann dynamics is given by a classical chaotic Hamiltonian with isolated period orbits, whose quantization would yield a point like spectrum containing the E'_a s [6]. Other physical approaches are based on statistical mechanics [7, 8], superconformal invariance [9], supersymmetric quantum mechanics [10], etc (see [2, 11, 12] for recent reviews). An interesting related approach is the construction of a quantum mechanical potential containing in its spectrum the prime numbers [13].

The starting point of our work is the Hamiltonian $H_{BK} = xp$, proposed by Berry and Keating, which reproduces at the semiclassical level the smooth part of the Riemann's formula giving the number of non trivial zeros below a given number, E [14, 15]. This Hamiltonian is formal since a consistent quantization has not yet been found. In this paper we shall propose a solution of this problem defining xp on a lattice. This is achieved working, not with xp , but with its inverse $1/xp$, which turns out to be related to a class of QM models with limit cycles, or rather centers, in the Renormalization Group (RG).

The idea that the RG may have limit cycles was first considered by Wilson in 1971 [16], however at the time no models with this behavior were known. In the last few years limit cycles in the RG have been discovered in various models in several physical contexts, including nuclear physics [17], quantum field theory [18, 19], quantum mechanics [20], superconductivity [21, 22], Bose-Einstein condensation [23], effective low energy QCD [24], S-matrix models [25, 26], few body systems and Efimov states [17, 27], etc (for a review of see [27]). The subject of duality cascades in supersymmetric gauge theory [28] is also suggestive of limit-cycle behavior. The possibility of chaotic flows has also been recently considered [20, 29].

The relevant model for this work is the, so called, Russian doll BCS model of superconductivity, and specially its QM version [21, 22]. In the RD model the standard pairing coupling g flows periodically with the scale, a fact that is intimately related to the existence of a series of bound states of two electrons (Cooper pairs) whose energies scale as $e^{-n\lambda}$ ($n = 0, 1, 2, \dots$), where λ is the period of the RG cycles. These bound states have a size that scales as $e^{n\lambda}$ ($n = 0, 1, 2, \dots$) which is the reason for calling them Russian dolls, by analogy with the popular matrioskas. The RG period is the main feature of a RG with limit cycles. In the RD model it is given by $\lambda = 2\pi/h$, where h is a coupling in the Hamiltonian that breaks the time reversal symmetry.

Why should this model be related to the Hamiltonian xp which seems so far apart? Some hints lie on the following observations. In the RD model the wave function of a Cooper pair with energy E is given approximately by $\psi(n) \sim 1/(n - E)^{1-ih}$, where $n = 1, 2, \dots, N$ label the energy levels of the electron pairs. Since in this model the energies E_n converge towards zero, $E_n \sim e^{-n\lambda}$, there exist a bound state with $E = 0$, whose wave function is $\psi(n) \sim 1/n^{1-ih}$. This form recalls the Dirichlet series of the zeta function, $\zeta(s) = \sum_n 1/n^s$, with $s = 1 - ih$. The latter sum is the interaction term that is multiplied by the coupling g . Apparently, the RD model should be connected to $\zeta(1 - ih)$ rather than to $\zeta(1/2 - iE)$. It is worth to mention that in the cyclic sine Gordon model, which also has a cyclic RG, the zeta function $\zeta(1 - ih)$ appears in the expression of the effective central charge, where h is related to the period of the RG cycles as $\lambda = \pi/h$ [19, 25].

The situation is different in the BK model where the formal eigenfunctions of the normal ordered Hamiltonian $(xp + px)/2$ are given by $\psi(x) = 1/x^{1/2-iE}$, that resembles the Dirichlet series of $\zeta(1/2 - iE)$. Compare to this, the RD wave function with $E = 0$ has in the exponent of n the factor 1 instead of 1/2, and the imaginary part is fixed to a constant h instead of being energy dependent. We shall show in this paper that these two problems can be solved at once by relating the BK and the RD models by means of a third model whose classical Hamiltonian is simply the inverse of the BK one, namely $1/xp$. In a deep sense, the BK and the RD models turn out to be the two faces of the same coin.

The organization of the paper is as follows. In section II we review the BK and the RD models. We also define the inverse model based on $1/xp$ and discuss its relation with the previous ones. In section III we solve the inverse model in the continuum limit. In section IV we study its renormalization showing the existence of RG cycles and their connection

with the continuous solution. In section V we give its exact solution, derive the smooth part of the Riemann counting formula and present a numerical analysis. In section VI we generalize the inverse model and begin to study its properties. We state the conclusions and prospects in section VII.

II. THE HAMILTONIANS

In this section we introduce the Hamiltonians of the Berry-Keating model, the inverse model (\mathcal{I}) and the Russian doll model, and study their relations which can be represented symbolically as

$$BK \rightarrow \mathcal{I} = BK^{-1} \rightarrow RD \quad (1)$$

Before presenting the details, we shall start with an overview.

As we explained above, the classical version of the Berry-Keating Hamiltonian H_{BK} is the product xp , where x and p are the position and momentum of a particle moving in one dimension. H_{BK} fullfills some of the assumptions of the quantum chaos approach to the RH, particularly the breaking of time-reversal symmetry, to accomodate the GUE hypothesis and suggestive analogies involving the zeta function, the trace formula, the Riemann-Siegel formula, etc. The BK proposal has however remained at a speculative level since a consistent QM model of xp has not been constructed in so far.

To solve this problem we shall define the Hamiltonian H_I , which at classical level is the inverse of the BK Hamiltonian, namely $1/xp$. It would seem that nothing is gained by this trick. Nevertheless, a consistent QM model can be constructed by quantizing $1/xp$ on a lattice. The key observation is that the inverse of the momentum operator $p = -i\hbar d/dx$ is the 1D Green function $\frac{i}{\hbar}G(x, x') = \frac{i}{2\hbar}\text{sign}(x-x')$, where $\text{sign}(x)$ is the sign function. We shall define a regularized lattice version of the operator p^{-1} as the matrix $P_{n,m}^{-1} = \frac{i}{2\hbar}\text{sign}(n-m)$, where n and m run over the integers $1, 2, \dots, N$. The quantization of the position operator x is the diagonal matrix $X_{n,m} = n\delta_{n,m}$. In this construction the Hamiltonian H_I acts on a discrete Hilbert space of dimension N .

It will be important to study the behaviour of H_I under the Renormalization Group transformation which integrates the highest energy level reducing the size of the system to $N-1$. For the model to be renormalizable one needs an extra term with coupling constant

g_I . The other coupling constant, $h_I = 1/\hbar$, multiplies the term containing $P_{n,m}^{-1}$. Hence the \mathcal{I} model depends on two couplings constants h_I and g_I . Under the RG transformations h_I remains invariant, while g_I flows periodically with the scale. This periodicity is in turn related to the spectrum of the \mathcal{I} model.

The third Hamiltonian is the QM Russian doll Hamiltonian, which is a generalization of the standard BCS model of superconductivity having a cyclic RG. The RD Hamiltonian H_{RD} also depends on two coupling constants g_D and h_D , where h_D multiplies a time-reversal breaking term, proportional to $P_{n,m}^{-1}$, while g_D multiplies the familiar s -wave pairing interaction of the BCS model which preserves the time-reversal symmetry. The spectrum of this model has a series of bound and antibound states with Russian doll scaling. The RD model is brought in due to its close relationship with the \mathcal{I} model. Indeed, we shall show that each eigenstate of the \mathcal{I} model coincides with the zero energy bound state of an associated RD model. This bound state appears at the threshold of that model. From the RG viewpoint these two models will also be related.

A. The Berry-Keating model

The classical BK Hamiltonian [14, 15]

$$H_{BK}^{\text{cl}} = xp, \quad (2)$$

has classical trajectories given by the hyperbolas

$$x(t) = x_0 e^t, \quad p(t) = p_0 e^{-t}. \quad (3)$$

The dynamics is unbounded and one should not expect a discrete spectrum at the quantum level. Despite of that, Berry and Keating regularized the model introducing the Planck cell in phase space with sides l_x, l_p and area $h = l_x l_p$, such that $|x| > l_x$ and $|p| > l_p$ [14]. They computed the number of states $N_{BK}(E)$, with an energy below E , using the semiclassical formula

$$N_{BK}(E) = \frac{A(E)}{h} = \frac{1}{h} \int_{l_x}^{E/l_p} dx \int_{l_p}^{E/x} dp + \dots \quad (4)$$

where $A(E)$ is the area of the region $l_x < x < E/l_p$, $l_p < p < E/l_x$, $xp < E$ (see fig.1a). The result is

$$N_{BK}(E) = \frac{E}{\hbar} \left(\log \frac{E}{\hbar} - 1 \right) + 1 + \dots \quad (5)$$

Taking into account a Maslov phase $-1/8$, BK finally obtain

$$N_{BK}(E) = \frac{E}{2\pi} \left(\log \frac{E}{2\pi} - 1 \right) + \frac{7}{8} + \dots \quad (6)$$

where the energy E is measured in units of \hbar . Eq.(6) agrees with the asymptotic expansion of the smooth part of the Riemann counting formula of the non trivial zeros of the zeta function

$$N_{sm}(E) = \frac{1}{\pi} \text{Im} \log \Gamma \left(\frac{1}{4} + \frac{i}{2} E \right) - \frac{E}{2\pi} \log \pi + 1. \quad (7)$$

This expression is π^{-1} times the phase of the zeta function $\zeta(1/2 + iE)$ [30]. The non trivial zeros, ρ , are known to lie in the critical strip $0 < \text{Re}(\rho) < 1$. The number of them, $N(E)$, in the range $0 < \text{Im}(\rho) < E$, is given by the Riemann formula,

$$N(E) = N_{sm}(E) + N_{osc}(E), \quad (8)$$

where the oscillatory part depends of the zeta function on the critical line,

$$N_{osc}(E) = \frac{1}{\pi} \text{Im} \log \zeta \left(\frac{1}{2} + iE \right) \quad (9)$$

and it is of order $\log E$ [31]. The derivation of eq.(6) is heuristic and, to our knowledge, has not been reproduced from the quantization of the BK Hamiltonian. Bhaduri et al. [30] obtained eq.(7), up to some factor, studying the inverted harmonic oscillator Hamiltonian $p^2 - x^2$, which is related by a canonical transformation to xp . They employed a phase shift approach instead of the semiclassical bound state approach.

The BK work was motivated by Connes's work to prove the RH using p-adic numbers. This is known as the adelic approach to the RH and it is based on the construction of an abstract space where acts an hermitean operator, whose eigenvalues are the non trivial zeros of the zeta function [31]. The truth of the RH lies in the proof of a certain classical trace formula. Connes has also considered the operator xp in the adelic theory. The regularization

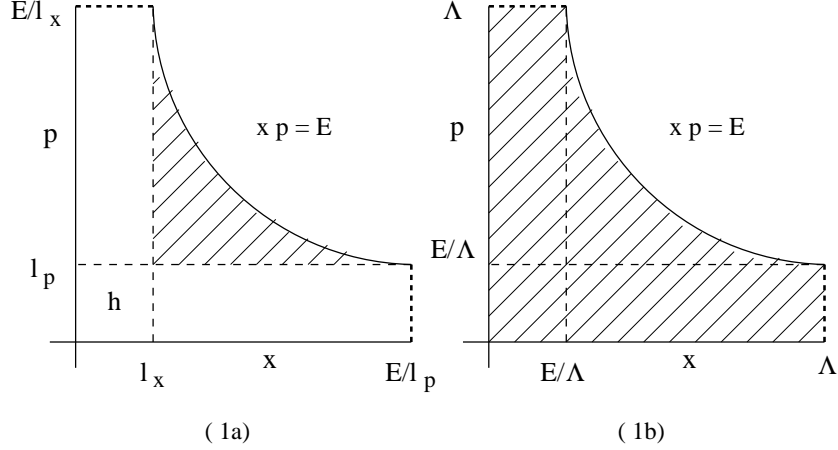


FIG. 1: 1a) The region in shadow is the phase space considered by Berry and Keating in the semiclassical computation of the number of states of the xp Hamiltonian (see eq.(4)). 1b) The shadow region gives the phase space considered by Connes (see eq.(10)).

is not the Planckian cell, but a standard cutoff in phase space given by $|x| < \Lambda$, $|p| < \Lambda$. The number of states in the region $0 < x < \Lambda$, $0 < p < \Lambda$, $xp < E$ (see fig.1b)

$$N_{Co}(E) = \frac{1}{h} \left[2E - \left(\frac{E}{\Lambda} \right)^2 + \int_{E/\Lambda}^{\Lambda} dx \int_{E/\Lambda}^{E/x} dp + \dots \right] \quad (10)$$

yields,

$$N_{Co}(E) = \frac{E}{2\pi} \log \Lambda^2 - \frac{E}{2\pi} \left(\log \frac{E}{2\pi} - 1 \right) + \dots \quad (11)$$

where E is measured in units of \hbar . There are important differences between eqs.(11) and (6). In Connes's formula the number of states diverges with the cutoff. There is also a negative sign of the term in (11), associated to the asymptotic Riemann formula, as compared with the BK formula (6). According to Connes, this negative sign agrees with the overall sign in a formal expression of $N_{osc}(E)$ obtained using the Euler product formula of $\zeta(1/2+iE)$ into (9) [31]. These results imply that the Riemann zeros, in the adelic approach, are missing states in a continuum spectrum. The physical picture is that of white light with dark absorption lines labelled by the zeros of the zeta function. Using this analogy, the Riemann zeros, according to BK, would be emission lines. Our results are along the lines of Connes, as we shall show.

We shall end this brief review of the BK approach by giving the formal hermitian operator which corresponds to (2),

$$H_{BK} = \frac{1}{2}(xp + px) = -i\hbar \left(x \frac{d}{dx} + \frac{1}{2} \right). \quad (12)$$

whose formal eigenfunctions are

$$\psi_E(x) = \frac{A}{x^{1/2 - iE/\hbar}}. \quad (13)$$

As noticed by BK, the wave function contains the power x^{-s} which appears in the Dirichlet series for $\zeta(s)$ and the Euler product, although those formulas are convergent only in the region $Re(s) > 1$, while in eq.(13) $s = 1/2 - iE/\hbar$, which lies outside. The rest of the BK paper discusses possible quantum boundary conditions that could generate the Riemann zeros. The guiding idea is that xp is the generator of the scale transformations in phase space, a fact that also plays a role in Connes's work.

Generalization of the BK model

The Hamiltonian (2) can be generalized to the form $v(x)p$, where $v(x)$ is a generic function which we shall assume is positive and monotonically increasing for $x > 0$. The classical evolution equation $\dot{x} = v(x)$, implies that $v(x)$ is the velocity of the particle. The semiclassical formula for the number of states à la Connes gives

$$N_{Co}(E) = \frac{E}{2\pi} \int_{v^{-1}(E/\Lambda)}^{\Lambda} \frac{dx}{v(x)} + \frac{\Lambda}{2\pi} v^{-1}(E/\Lambda), \quad (14)$$

where v^{-1} is the inverse function of $v(x)$. If $v(x) = x$, eq.(14) becomes eq.(11). Similarly, the formal Hamiltonian associated to vp

$$H_{BK} = \frac{1}{2}(v(x) p + p v(x)) = -i\hbar \left(v(x) \frac{d}{dx} + \frac{1}{2} v'(x) \right), \quad (15)$$

has formal eigenfunctions

$$\psi_E(x) = \frac{A}{v(x)^{1/2}} \exp \left(\frac{iE}{\hbar} \int_{x_0}^x \frac{dx'}{v(x')} \right). \quad (16)$$

If $v(x) = x$ we recover (13).

B. The inverse Hamiltonian

The inverse of the generalized BK Hamiltonian (15) is

$$H_{BK}^{-1} = v^{-1/2} p^{-1} v^{-1/2}, \quad (17)$$

where we use the normal ordering $v^{1/2} p v^{1/2}$ of H_{BK} , which is equivalent to (15). By assumption $v(x) > 0$ for $x > 0$, then the square root of $v(x)$ is real. For this and other reasons we shall work on the half line $x > 0$. The inverse of the momentum operator p is

$$\langle x|p^{-1}|x'\rangle = \frac{i}{\hbar}G(x, x') = \frac{i}{2\hbar} \text{sign}(x - x'), \quad (18)$$

where $G(x, x')$ is the 1D Green function associated to d/dx and $\text{sign}(x)$ is the sign function. The advantage of using H_{BK}^{-1} instead of H_{BK} is that the former operator can be easily regularized on a 1D lattice due to the simplicity of the 1D Green function. The lattice version of the formal Hamiltonian (17) is the N -dimensional matrix

$$\langle n|H_I|m\rangle = \frac{1}{2}f_n (g_I + ih_I\text{sign}(n - m)) f_m, \quad (19)$$

where $n, m = 1, 2, \dots, N$ and

$$h_I = \frac{1}{\hbar}, \quad f_n = \frac{1}{\sqrt{v_n}}. \quad (20)$$

H_I contains an extra term with coupling constant g_I , which is needed for renormalization (see section IV). The *pure* BK model corresponds to the case $g_I = 0$, but we shall also consider non vanishing values of g_I . The regularized BK Hamiltonian will then be defined as the inverse of H_I , namely

$$H_{BK}^{(\text{reg})}(v_n, g_I, \hbar) = H_I^{-1}(f_n, g_I, h_I) \quad (21)$$

In the case where $g_I = 0$, one gets

$$H_{BK}^{(\text{reg})}(v_n, g_I = 0, \hbar) = v(X)^{1/2} P v(X)^{1/2}, \quad (22)$$

where X and P^{-1} are the N dimensional matrices

$$\langle n|X|m\rangle = n\delta_{n,m}, \quad \langle n|P^{-1}|m\rangle = \frac{i}{2\hbar}\text{sign}(n - m). \quad (23)$$

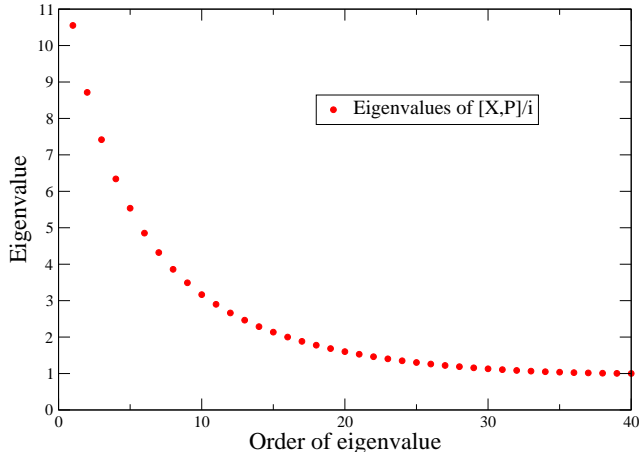


FIG. 2: Eigenvalues of the commutator $[X, P]/i$ ($\hbar = 1$) for $N = 50$. We display 40 eigenvalues which converge towards 1. The remaining ones are larger in absolute value. The sum of all the eigenvalues is zero as a consequence of the vanishing of the trace of $[X, P]$.

For N an even number, the matrix P^{-1} is not singular and its inverse is given by

$$\langle n|P|m\rangle = -2\hbar i (-1)^{n+m} \text{sign}(n - m). \quad (24)$$

X and P do not satisfy the canonical commutation relation $[x, p] = i\hbar$. The trace of the LHS of the commutator is zero while on the RHS is $i\hbar N$. This is the textbook argument to show that the Heisenberg's indetermination relation cannot be realized by finite dimensional matrices. Nevertheless, most of the eigenvalues of $[X, P]/i$ converge towards \hbar (see fig.2). From this result we expect to recover the formal BK model in the continuum limit of the discrete Hamiltonian (22). Since $[X, P] \neq i\hbar$, the Hamiltonian (22) cannot be written as $1/2(v(X)P + Pv(X))$, but this fact is unimportant. We can then work either with the Hamiltonians (19) or (22). We shall choose the former for convenience.

The g_I interaction has a classical version. This term is non local in x -space and ultralocal in p -space. By dimensional reasons it should be proportional to $\delta(p)$, yielding $H_I^{\text{cl}} = (1/p + \delta(p)g_I/2)/v(x)$, whose inverse is again $pv(x)$ (recall that $p \delta(p) = 0$). At the quantum level g_I does play a role in $H_{BK}(g_I) = H_I^{-1}(g_I)$ setting the boundary conditions.

The operator $K = h/xp$ was used by BK to implement a canonical transformation $x \rightarrow x_1 = h/p$, $p \rightarrow p_1 = xp^2/h$, named *quantum exchange* by the h dependence [14]. Berry and Keating, tried to combine the dilatation and the quantum exchange symmetries, to generate

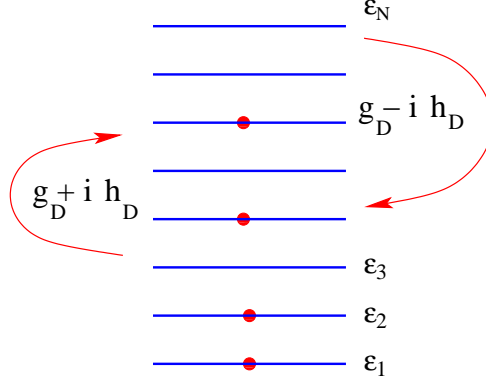


FIG. 3: Pictorial representation of the RD model. The horizontal lines represent the energy levels ε_n ($n = 1, \dots, N$). The dots are pairs of electrons occupying a doubly degenerate state. The arrows give the transitions among levels induced by the interactions in the Hamiltonian (25).

the Riemann zeros. In our case, the operators xp and $1/xp$ are used as Hamiltonians and not as symmetries.

H_I has two properties which simplifies its study: it is renormalizable and exactly solvable for all values of the coupling constants h_I, g_I and f_n . One can find an analytic form of the exact eigenvectors and an explicit equation for the eigenenergies. These properties are reminiscent of the Bethe ansatz, as it is indeed the case.

C. The Russian doll Hamiltonian

A Hamiltonian closely related to H_I is [21]

$$\langle n | H_{RD} | m \rangle = \varepsilon_n \delta_{n,m} - \frac{1}{2} (g_D + i h_D \text{sign}(n - m)), \quad (25)$$

where ε_n, g_D, h_D are real parameters. In physical applications ε_n , are the kinetic energies of pairs of electrons occupying doubly degenerate levels in the conduction band of a metal. The term proportional to g_D is a pairing interaction due to the phonon exchange in the s -wave channel, which leads to the formation of Cooper pairs if $g_D > 0$. The model with $h_D = 0$ was first considered by Cooper and it was the precursor of the Bardeen-Cooper-Schrieffer model of superconductivity [32, 33].

The coupling h_D was introduced in reference [21], motivated by the work of Glazek and Wilson, who proposed an extension of the well known 2D delta function potential in order to

show the existence of RG limit cycles in a simple QM model [20]. The QM Russian doll model (25), together with its many body version, also have a cyclic RG, which has been studied in detail in references [21, 22]. The exact solution was obtained in [34] using algebraic Bethe ansatz methods, showing that the RD model is nothing but an inhomogenous XXX vertex model with a boundary operator. In the vertex formulation the coupling h_D parameterizes the quantum Yang-Baxter matrix, the coupling g_D parameterizes the boundary operator and the energy levels ε_n give the inhomogenities. The most natural choice of the energy levels is $\varepsilon_n = n$, in units of twice the electronic level spacing. The equally spaced BCS model for a finite and small number of energy levels have been studied intensively due to the fabrication of ultrasmall metallic grains (see [35] for a review). This model is also relevant in Nuclear Physics, where it is known as the picket fence model, and in other potential applications in Quantum Optics, and dilute Fermi-Bose gases (see [36] for a review). Up to date it is not known wether the RD-BCS model of superconductivity explains some physical system existing in Nature or in the Lab. A possible reason is that the h_D coupling breaks the time reversal symmetry, while the microscopic laws of Nature do not. However, this symmetry can be broken spontaneously or explicitly by the action, for example, of magnetic fields.

We shall next show the relation between the RD and the \mathcal{I} models. Let's first compare their Schrödinger equations,

$$H_I \psi = E_I \psi, \quad H_{RD} \phi = E_{RD} \phi, \quad (26)$$

which read explicetly

$$E_I \psi_n = \frac{1}{2} \sum_{m=1}^N f_n (g_I + i h_I \text{sign}(n - m)) f_m \psi_m \quad (27)$$

$$(\varepsilon_n - E_{RD}) \phi_n = \frac{1}{2} \sum_{m=1}^N (g_D + i h_D \text{sign}(n - m)) \phi_m. \quad (28)$$

Given an eigenstate, ψ , of the \mathcal{I} model let us define the wave function

$$\phi_n = f_n \psi_n, \quad (29)$$

writting (27) as

$$\frac{1}{f_n^2} E_I \phi_n = \frac{1}{2} \sum_{m=1}^N (g_I + i h_I \text{sign}(n - m)) \phi_m. \quad (30)$$

If $E_I \neq 0$, and dividing eq.(30) by E_I , one obtains eq.(28) with $E_{RD} = 0$. This leads to the identifications:

$$\varepsilon_n = \frac{1}{f_n^2}, \quad g_D = \frac{g_I}{E_I}, \quad h_D = \frac{h_I}{E_I}, \quad (31)$$

which establish a map from the spectrum of the \mathcal{I} model into a collection of RD models which have in common the energy values, ε_n , focusing on the $E_{RD} = 0$ state, while varying the couplings g_D and h_D according to E_I . Moreover, eqs.(20) establish a link between the regularized BK model and the RD model, Combining (31) with (20) we get

$$\varepsilon_n = v_n, \quad h_D = \frac{E}{\hbar}, \quad (32)$$

where $E = 1/E_I$ is an eigenvalue of $H_{\text{BK}} = H_I^{-1}$. Let us remark that the transformation (29) is non unitary. For the model $\varepsilon_n = n$ and in the limit $N \rightarrow \infty$, ϕ_n will be a normalizable wave function, corresponding to a bound state, but ψ_n will not, as corresponds to a scattering state.

The map $\text{BK} \rightarrow \text{RD}$ is quite remarkable. It implies that the spectrum of the BK Hamiltonian can be found by looking at the zero energy bound states of a RD model where the h_D coupling is fine tuned according to the energy of the state. In this mapping, the velocities v_n become energy levels ε_n . In particular, the choice $v = x$ corresponds to the equally space model $\varepsilon_n = n$, which is the common choice for physical applications [35, 36].

The correspondence (32) can be easily derived at the classical level. Take $g_D = 0$ for simplicity. The classical energy (25) is $E_{RD} = \varepsilon(x) - h_D/p$ (with $\hbar = 1$). Setting $E_{RD} = 0$ one finds $p \varepsilon(x) = h_D$, which is the classical energy of the BK model with $v(x) = \varepsilon(x)$ and $E = h_D$.

In summary, we have constructed a consistent quantum model which generalizes the BK Hamiltonian xp by means of the inverse model I , whose spectrum can be mapped into the zero eigenstates of associated RD models. As we shall see this connection is the key of the renormalizability and solvability of the BK model so defined.

III. CONTINUUM LIMIT

The three models described in the previous section can be solved exactly. However it is worth to solve them first in the limit where the lattice size N is very large. In this limit the

discrete variable n will be considered as continuous and varying in the interval $1 \leq n \leq N$. The Schrödinger eq.(27) becomes,

$$E_I \psi(n) = \frac{1}{2} \int_1^N dm f(n)(g_I + ih_I \text{sign}(n - m))f(m)\psi(m), \quad (33)$$

where $\psi(n)$ and $f(n)$ are continuous functions. To solve (33) we use again the change of variables (29),

$$\varepsilon(n)\phi(n) = \frac{1}{2} \int_1^N dm (g_D + ih_D \text{sign}(n - m))\phi(m), \quad (34)$$

where $\varepsilon(n), g_D$ and h_D are given by eqs.(31). As shown above, eq.(34) is satisfied by an eigenstate of the RD model with $E_{RD} = 0$, and can be solved in the same way as was done in references [21, 22]. Taking the derivative with respect to n yields

$$\frac{d}{dn} [\varepsilon(n)\phi(n)] = ih_D \phi(n), \quad (35)$$

whose integral determines the functional form of $\phi(n)$,

$$\phi(n) = \frac{A}{\varepsilon(n)} \exp \left(ih_D \int_1^n \frac{dn'}{\varepsilon(n')} \right). \quad (36)$$

Using eqs.(31) and (32) this leads to

$$\psi_E(n) = \frac{A}{\varepsilon(n)^{1/2}} \exp \left(\frac{iE}{\hbar} \int_1^n \frac{dn'}{\varepsilon(n')} \right). \quad (37)$$

which coincides with the wave function (16) for the generalized BK model. This result agrees with the fact that the commutator $[X, P]$ converges asymptotically to $i\hbar$ (see fig.2). To find the eigenenergies $E = 1/E_I$ let us consider eq.(34) at the boundaries of the interval, $n = 1, N$

$$\begin{aligned} \varepsilon(1)\phi(1) &= \frac{1}{2}(g_D - ih_D) \int_1^N dn \phi(n) \\ \varepsilon(N)\phi(N) &= \frac{1}{2}(g_D + ih_D) \int_1^N dn \phi(n). \end{aligned} \quad (38)$$

Dividing both eqs,

$$\frac{g_D + ih_D}{g_D - ih_D} = \frac{\varepsilon(N)\phi(N)}{\varepsilon(1)\phi(1)}, \quad (39)$$

and using (36), one finds

$$\frac{g_D + ih_D}{g_D - ih_D} = \exp \left(ih_D \int_1^N \frac{dn}{\varepsilon(n)} \right), \quad (40)$$

or equivalently

$$\frac{g_I + ih_I}{g_I - ih_I} = \exp \left(\frac{iE}{\hbar} \int_1^N \frac{dn}{\varepsilon(n)} \right). \quad (41)$$

The eigenenergies are obtained taking the log

$$N_I(E) = \frac{E}{2\pi\hbar} \int_1^N \frac{dn}{\varepsilon(n)} - \frac{\alpha}{\pi}, \quad (42)$$

with

$$\alpha = \text{Arctan} \left(\frac{h_I}{g_I} \right) \quad (43)$$

and where $N_I = 0, \pm 1, \pm 2, \dots$ label the eigenstates. In the case $\varepsilon(n) = n, g_I = 0$, (42) reduces to

$$N_I(E) = \frac{E}{2\pi\hbar} \log N - \frac{1}{2} \quad (44)$$

which yields an equally space spectrum symmetric around zero energy,

$$\frac{E_n}{\hbar} = \frac{2\pi}{\log N} (n + 1/2), \quad n = 0, \pm 1, \dots \quad (45)$$

In the limit $N \rightarrow \infty$, this spectrum becomes a continuum with constant energy level density. The conclusion is that the regularized BK model does not have a discrete spectrum whose eigenenergies could be identified with the Riemann zeros or an approximation to them. On the other hand, eq.(44) agrees with the leading term in Connes's formula (11), which also diverges with the cutoff Λ .

The wave function (37) in the case $\varepsilon(n) = n$ is

$$\psi_E(n) = \frac{A}{n^{1/2 - iE/\hbar}}, \quad (46)$$

which agrees with the BK wave function (13). This is the wave function of a free particle moving in a box of length $L_N = \log N$. Indeed, let us define the coordinate

$$q \equiv \log n, \quad 0 \leq q \leq L_N = \log N, \quad (47)$$

and the momentum variable

$$k \equiv \frac{E}{\hbar}, \quad k_n = \frac{2\pi}{L_N} \left(n + \frac{1}{2} \right). \quad (48)$$

The scalar product of two eigenstates (46) with quantum numbers n_1 and n_2 is

$$\langle \psi_{E_{n_1}} | \psi_{E_{n_2}} \rangle = A^2 \int_1^N \frac{dn}{n} n^{i(E_{n_1} - E_{n_2})/\hbar} = A^2 \int_0^{L_N} dq e^{2\pi i q (n_1 - n_2)/L_N} = \delta_{n_1, n_2}, \quad (49)$$

where $A = L_N^{-1/2}$ is a normalization constant. Notice that the plane waves satisfy antiperiodic boundary conditions, which can be changed by choosing $g_I \neq 0$. In particular, $g_I = \infty$ yields periodic BC's.

The variable q can be defined for generic choices of levels $\varepsilon(n)$

$$q(n) = \int_1^n \frac{dn'}{\varepsilon(n')}, \quad 0 \leq q \leq L_N = \int_1^N \frac{dn'}{\varepsilon(n')}. \quad (50)$$

The momenta k is still defined by (48). The eigenenergies E , or rather momenta $k = E/\hbar$, satisfy (41), which can be written as

$$e^{2i\alpha} = e^{ikL_N}. \quad (51)$$

This is the quantization condition of a free particle moving in a box of length L_N , with twisted boundary conditions fixed by α . We give below a RG interpretation of q .

IV. RENORMALIZATION GROUP ANALYSIS

The Hamiltonian H_I is renormalizable in the sense that upon integration of the high energy degrees of freedom, the effective Hamiltonian governing the dynamics of the remaining variables coincides with the original one parameterized by new coupling constants. For a discrete QM model the RG procedure consists in the Gauss elimination of the highest energy degree of freedom and its replacement into the Schrödinger eq. for the other variables (one can also eliminate the lowest energy component in which case the flow goes towards the ultraviolet) [20]. Let us describe this process for H_I . We start from eq.(27) written as

$$(E_I - \frac{1}{2}g_I f_n^2)\psi_n = \frac{g_I + ih_I}{2} \sum_{m=1}^{n-1} f_n f_m \psi_m + \frac{g_I - ih_I}{2} \sum_{m=n+1}^N f_n f_m \psi_m. \quad (52)$$

Next we eliminate ψ_N in terms of $\psi_{n < N}$

$$\psi_N = \frac{g_I + ih_I}{2E_I - g_I f_N^2} \sum_{m=1}^{N-1} f_N f_m \psi_m. \quad (53)$$

Plugging this equation back into (52), for $n < N$, one obtains a system of equations for the variables $\psi_{n < N}$, which is identical to the original system (52) except that the couplings are

$$g'_I = g_I + \frac{g_I^2 + h_I^2}{2E_I f_N^{-2} - g_I}, \quad (54)$$

$$h'_I = h_I, \quad (55)$$

$$f'_n = f_n \quad (n = 1, \dots, N - 1). \quad (56)$$

Hence h_I and f_n are RG invariant couplings, while g_I changes under the RG. This is the reason to add the g_I coupling to the Hamiltonian H_I since it is generated by the RG.

The RD model (28) leads to an equation similar to eq.(54) for g_D , where the term $E_I f_N^{-2} = E_I \varepsilon_N$ is replaced by $\varepsilon_N - E_{\text{RD}}$, with E_{RD} the energy of the eigenstate. To study the low energy degrees of freedom, i.e. $|E_{\text{RD}}| \ll \varepsilon_N$, one can replace $\varepsilon_N - E_{\text{RD}}$ by ε_N , obtaining a RG equation for g_D which does not depend on E_{RD} . However, to analyze eq.(54) in the continuum, we cannot eliminate the term E_I , otherwise the scale dependence would disappear. We shall use instead the parametrization (31) to express g_I, h_I, f_N in terms of the couplings g_D, h_D, ε_N of the associated RD model. Eq.(54) implies for g_D

$$g'_D = g_D + \frac{g_D^2 + h_D^2}{2\varepsilon_N - g_D}, \quad (57)$$

where g_D and h_D must be regarded as functions of E_I , or $E = 1/E_I$. Eq.(57) is the exact RG equation associated to a state with zero energy in the RD model. This result is a consequence of the relation between the \mathcal{I} and RD models explained in section III. A pictorial representation of eq.(57) is given in fig. 4.

Let's analyze eq.(57) in the continuum limit as in the previous section. For weak couplings we get

$$g_D(N - 1) \simeq g_D(N) + \frac{g_D^2(N) + h_D^2}{2\varepsilon_N}, \quad (58)$$

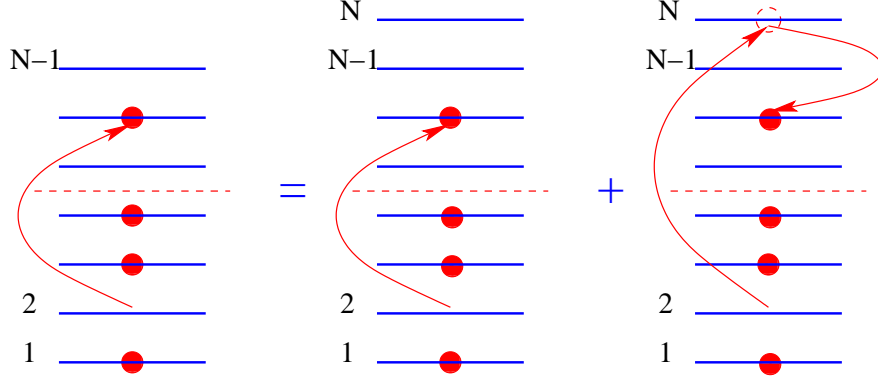


FIG. 4: Graphic representation of eq.(57). The term $g_D^2 + h_D^2$ arises from the tunneling of a pair of electrons from a level $n_i < N$ to the highest level N , followed by the decay to a level $n_f < N$. The denominator $2\varepsilon_N - g_D$ is a kinematical factor.

where $g_D = g_D(N)$ and $g'_D = g_D(N - 1)$ are regarded as a continuous function of N . A gradient expansion of $g_D(N)$ yields the differential eq.

$$\frac{dg_D}{dN} = -\frac{g_D^2 + h_D^2}{2\varepsilon_N}, \quad (59)$$

which for the uniform model becomes

$$\frac{dg_D}{ds} = \frac{1}{2}(g_D^2 + h_D^2), \quad (60)$$

where $N(s) = e^{-s}N$ is the system size at the scale s and $N(0) = N$ is the initial size of the system. In general, for a monotonically increasing function $\varepsilon(n)$, one can define the scaling variable s as

$$s(n) = \int_n^N \frac{dn'}{\varepsilon(n')}, \quad (61)$$

so that eq.(59) takes also the form of eq. (60). Comparison of eqs.(61) and (50) yields

$$s(n) = L_N - q(n), \quad (62)$$

which relates s to the variable q used in the previous section. The solution of (60) is

$$g_D(s) = h_D \tan \left(\frac{1}{2} h_D s + \text{Arctan} \left(\frac{g_D}{h_D} \right) \right), \quad (63)$$

therefore

$$g_I(s) = \frac{1}{\hbar} \tan \left(\frac{E}{2\hbar} s + \alpha \right). \quad (64)$$

The coupling $g_I(s)$ is periodic under the RG with a period

$$\lambda_E = \frac{2\pi}{h_D} = \frac{2\pi\hbar}{E}. \quad (65)$$

In the RD model the RG period of all the flows is the constant $2\pi/h_D$. However, (65), yields a RG period which depends on the energy of the state. This fact is related to the energy spectrum as we explain below.

Russian doll scaling: gapped versus gapless

Let us consider the n^{th} state $E_n(N)$ given by eq.(42),

$$n = \frac{E_n(N)}{2\pi\hbar} \int_1^N \frac{dm}{\varepsilon(m)} - \frac{\alpha}{\pi}. \quad (66)$$

After a RG cycle the size is reduced from N to $N(\lambda_n)$ (recall eqs.(65) and (61)),

$$\lambda_n = \frac{2\pi\hbar}{E_n(N)} = \int_{N(\lambda_n)}^N \frac{dm}{\varepsilon(m)}, \quad (67)$$

so

$$1 = \frac{E_n(N)}{2\pi\hbar} \int_{N(\lambda_n)}^N \frac{dm}{\varepsilon(m)}. \quad (68)$$

Splitting the interval of integration $(1, N)$ in eq.(66) into the intervals $(1, N(\lambda_n)) \cup (N(\lambda_n), N)$, and using (68) one gets

$$n - 1 = \frac{E_n(N)}{2\pi\hbar} \int_1^{N(\lambda_n)} \frac{dm}{\varepsilon(m)} - \frac{\alpha}{\pi}. \quad (69)$$

This equation has the same form as eq.(66) with the replacements $n \rightarrow n-1$ and $N \rightarrow N(\lambda_n)$, which implies,

$$E_n(N) = E_{n-1}(N(\lambda_n)). \quad (70)$$

In the uniform case $\varepsilon_n = n$, $g_I = 0$ one has

$$\lambda_n = \frac{\log N}{n + 1/2}, \quad N(\lambda_n) = e^{-\lambda_n} N = N^{\frac{n-1/2}{n+1/2}}, \quad (71)$$

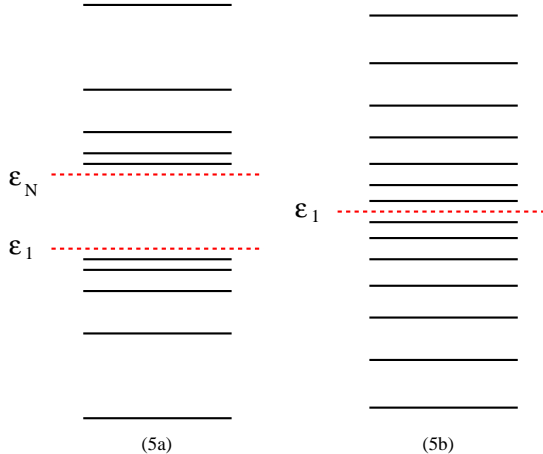


FIG. 5: 5a) Energy levels of the RD model. The bound states lie below the lowest energy ε_1 , while the antibound states lie above the highest energy ε_N . There are also states within the energy band $(\varepsilon_1, \varepsilon_N)$ (not depicted). The scaling is exponential (see eq.(74)). 5b) Energy levels $E_{I,n} = 1/E_n$ of the \mathcal{I} model (see eq.(45)). The energies converge to the energy $\varepsilon_1 = 0$ as $\sim 1/|n|$, from above and below.

so

$$E_n(N) = E_{n-1}(N^{\frac{n-1/2}{n+1/2}}), \quad (72)$$

which can be readily verified using eq.(45). In the usual RD model the RG period is the constant $\lambda_D = 2\pi/h_D$, which does not depend on the energy of the states. The analogue of scaling relation (72) is

$$E_n(N) = E_{n-1}(e^{-\lambda_D} N). \quad (73)$$

This relation leads to an exponential decaying behaviour of the bound state energies

$$E_n(N) \sim N e^{-n\lambda_D}, \quad (74)$$

which is in sharp contrast with the linear decaying of the energies $E_{I,n} = 1/E_n$ in the \mathcal{I} -model (see eq. (45)), which reflects the gapless nature of its spectrum (see fig.5).

Counting RG cycles

In a finite system the number of RG cycles is of course finite. In the RD model this number is given approximately by [21, 22]

$$n_c \sim \frac{h_D}{2\pi} \log N. \quad (75)$$

The reason for (75) is that after each cycle the system size is reduced by a factor $e^{-\lambda_D}$ where $\lambda_D = 2\pi/h_D$. Hence, the number of cycles n_c needed to reduce the system to one site satisfies $e^{-n_c \lambda_D} N \sim 1$, which leads to eq.(75). This eq. also gives the number of bound states of the model, due to the one-to-one correspondence between RG cycles and bound states (recall (73)).

For the uniform \mathcal{I} -model we expect the formula (75) to give the number of RG cycles for the appropriate value of h_D as a function of E_n , namely

$$n_c(E_n) \sim \frac{E_n}{2\pi\hbar} \log N = n + 1/2. \quad (76)$$

Iterating eq.(72) one can compute the size of the system after n_c RG cycles,

$$N \rightarrow N^{\frac{n-1/2}{n+1/2}} \rightarrow N^{\frac{n-3/2}{n+1/2}} \rightarrow \dots \rightarrow N^{\frac{n+1/2-n_c}{n+1/2}} \sim 1. \quad (77)$$

Hence the integer n , labelling the state E_n , coincides roughly with the number of RG cycles n_c needed to reduce the system to one site. This result is exact to leading order in N , but as we shall see below there are finite size corrections which will play an important role in the discussion.

V. EXACT SOLUTION

The discrete Schrödinger eq.(27) can be solved in a very simple way which parallels the derivation done in the section III. This solution coincides with the exact Bethe ansatz solution of the RD model found in reference [34] for a single Cooper pair. There is another derivation of the exact solution using the RG method of Glazek and Wilson [22]. The idea is to keep the energy E in the Gauss elimination procedure until the system size is one. That gives an exact equation for the eigenenergies E . The renormalizability of the model makes this procedure doable and that is the reason for its solvability.

As explained in section II, each state with energy E_I of the Hamiltonian (19) coincides with the zero energy state of the RD Hamiltonian (25) under the identifications (31). The equation of that state is given by (28) with $E_{RD} = 0$, i.e.

$$\varepsilon_n \phi_n = \frac{1}{2} \sum_{m=1}^N (g_D + ih_D \text{sign}(n - m)) \phi_m. \quad (78)$$

Subtracting the eqs. for ϕ_n and ϕ_{n+1}

$$\varepsilon_{n+1} \phi_{n+1} - \varepsilon_n \phi_n = \frac{ih_D}{2} (\phi_n + \phi_{n+1}), \quad (79)$$

gives a discrete differential equation, which is a recursion relation for ϕ_{n+1} as a function of $\varepsilon_n, \varepsilon_{n+1}$ and ϕ_n ,

$$\frac{\phi_{n+1}}{\phi_n} = \frac{\varepsilon_n + ih_D/2}{\varepsilon_{n+1} - ih_D/2}, \quad n = 1, \dots, N - 1. \quad (80)$$

A gradient expansion of ϕ_n and ε_n in (79) reproduces eq.(35). Iterating (80) yields

$$\frac{\phi_N}{\phi_1} = \prod_{n=1}^{N-1} \frac{\varepsilon_n + ih_D/2}{\varepsilon_{n+1} - ih_D/2}. \quad (81)$$

Eqs.(80) is a set of $N - 1$ equations while (78) contain N equations. Hence there is one more equation to impose. It is convenient to choose eqs.(78) at the two boundaries, $n = 1$ and N obtaining,

$$\begin{aligned} (\varepsilon_1 - ih_D/2) \phi_1 &= \frac{1}{2} (g_D - ih_D) \sum_{m=1}^N \phi_m \\ (\varepsilon_N + ih_D/2) \phi_N &= \frac{1}{2} (g_D + ih_D) \sum_{m=1}^N \phi_m. \end{aligned} \quad (82)$$

Dividing both eqs.

$$\frac{g_D + ih_D}{g_D - ih_D} = \frac{(\varepsilon_N + ih_D/2) \phi_N}{(\varepsilon_1 - ih_D/2) \phi_1}, \quad (83)$$

and using (81) gives

$$\frac{g_D + ih_D}{g_D - ih_D} = \prod_{n=1}^N \frac{\varepsilon_n + ih_D/2}{\varepsilon_n - ih_D/2}, \quad (84)$$

which can also be written as

$$\frac{g_I + ih_I}{g_I - ih_I} = \prod_{n=1}^N \frac{\varepsilon_n + iE/2\hbar}{\varepsilon_n - iE/2\hbar}, \quad (85)$$

where E is the energy of the BK Hamiltonian. The solutions of eq.(85) are obtained taking the log

$$N_I(E) = \frac{1}{2\pi i} \sum_{n=1}^N \log \left(\frac{\varepsilon_n + iE/2\hbar}{\varepsilon_n - iE/2\hbar} \right) - \frac{\alpha}{\pi} \in \mathbf{Z}, \quad (86)$$

where N_I is an integer labelling the eigenstates.

1) Completeness of the spectrum.

Let's write eq.(86) as

$$N_I(E) = \frac{1}{\pi} \sum_{n=1}^N \text{Arctan} \left(\frac{E}{2\hbar\varepsilon_n} \right) - \frac{\alpha}{\pi}. \quad (87)$$

The condition $\varepsilon_n = f_n^{-2} > 0, \forall n$ implies that $N_I(E)$ is a monotonically increasing function of E varying in the interval

$$-\frac{N}{2} - \frac{\alpha}{\pi} \leq N_I(E) \leq \frac{N}{2} - \frac{\alpha}{\pi}, \quad (88)$$

where $-\infty \leq E \leq \infty$. There are exactly N integers in the interval (88) corresponding to all the eigenvalues of H_{BK}^{reg} . For some choices of N and α one may eventually find a solution with $E = \infty$. If N is even all the solutions are finite.

2) The spectrum of the operator P

A particular example of BK Hamiltonian is given by the choice $v_n = \varepsilon_n = 1, g_I = 0$, which corresponds to the operator P (see eq.(22)). Its exact eigenvalues, p_n , follow immediately from eq.(87),

$$p_n = 2 \tan \left[\frac{\pi}{N} \left(n + \frac{1}{2} \right) \right], \quad -\frac{N}{2} \leq n < \frac{N}{2}, \quad (89)$$

which in the continuum limit coincide with the momenta of a free particle in a box with antiperiodic BC's, $p_n = \frac{2\pi}{N}(n + 1/2)$.

3) Relation with the continuum approximation.

The power expansion of the function Arctan in (87) is,

$$N_I(E) = \frac{E}{2\pi\hbar} \sum_{n=1}^N \frac{1}{\varepsilon_n} - \frac{\alpha}{\pi} + O(E^3). \quad (90)$$

In the continuum limit

$$\sum_{n=1}^N \frac{1}{\varepsilon_n} \rightarrow \int_1^N \frac{dn}{\varepsilon(n)}, \quad (91)$$

one recovers eq.(42). The higher order powers of E in (87) are multiplied by terms of the form $\sum 1/\varepsilon_n^{1+2m}$ with $m \geq 1$. In the case where $\varepsilon_n = n$ only the sum $\sum 1/\varepsilon_n \sim \log N$ diverges with N , which controls the large N limit of $N_I(E)$.

4) Continuum approximation of the exact solution

The previous discussion suggests to take the continuum limit directly in the exact equation (87), namely

$$N_I(E) \approx \frac{1}{\pi} \int_1^N dn \operatorname{Arctan} \left(\frac{E}{2\hbar\varepsilon(n)} \right) - \frac{\alpha}{\pi}. \quad (92)$$

In the uniform case, $\varepsilon(n) = n$, $\alpha = \pi/2$, and in the limit $N \gg |E|/2\hbar \gg 1$, eq.(92) becomes

$$N_I(E) \approx \frac{E}{2\pi\hbar} \log N - \frac{E}{2\pi\hbar} \left(\log \frac{|E|}{2\hbar} - 1 \right) + O(1). \quad (93)$$

The finite piece of this equation agrees with Connes's formula (11), except for a term linear in E , namely $E/(2\pi) \log \pi$. The origin of this term, in the Riemann counting formula, can be traced back from the expression (7), and it is due to a factor π^s appearing in the functional relation satisfied by $\zeta(s)$. The leading term $E/(2\pi) \log E$, as well as another linear term in E , come from the log of the Gamma function in (7).

The divergent terms in eqs.(93) and (11) have a similar form which depend on the respective cutoffs N and Λ . Let us suppose for a while that both cutoffs are related by the eq. $N = \pi\Lambda^2$. Then the divergent and the finite parts in both formulas agree. Notice that the π factor in the latter relation explains the missing factor $E/(2\pi) \log \pi$ in eq.(93). Unfortunately, the relation $N = \pi\Lambda^2$ does not seem to follow from the counting of states in both models. In the \mathcal{I} model this is given by N , while in the Connes model, at the semiclassical level, it would be given by Λ^2/π ($\hbar = 1$) corresponding to the phase space

($0 < x < \Lambda, -\Lambda < p < \Lambda$). This comparison gives $N = \Lambda^2/\pi$, rather than $N = \pi\Lambda^2$. In any case, the linear term $\propto E$, in both counting formulas, depends on the cutoffs and hence on the particular regularization chosen. Apparently, Connes's regularization and ours are different. In the next paragraph we shall consider a zeta function regularization of the model, which will shed further light on this issue.

Another interesting point concerns the spectroscopic interpretation of our results. As we said above they are along the lines of Connes's absorption picture. However it must be kept in mind that the eigenstates counted by the smooth part of the Riemann formula are not really missing in the whole spectra but shifted to higher energies because the interactions. This blueshift makes that in a range of energies, say $(0, E)$, there are less states than expected from the analysis of the continuum limit. In this sense, a more appropriate spectroscopic interpretation of our results will be in terms of a blueshift of energy levels, which are then missing in fixed energy intervals.

5) Exact solution in the uniform case.

Eq.(87) can be given an exact analytic formula in terms of known functions in the uniform case. We shall add a *zero point* contribution, a , to the energy levels, i.e.

$$\varepsilon_n = n + a, \quad n = 1, 2, \dots, N, \quad (94)$$

which does not modify the large N properties of N_I discussed above. It is more convenient to write (87) in the product form (85) ($\hbar = 1$)

$$e^{2\pi i N_I(E)} = e^{-2i\alpha} \prod_{n=1}^N \frac{\varepsilon_n + iE/2}{\varepsilon_n - iE/2}. \quad (95)$$

Inspired by (93), we shall define the finite part of N_I as

$$n_I(E) = \lim_{N \rightarrow \infty} \left(\frac{E}{2\pi} \log N - N_I(E) \right), \quad (96)$$

where a minus sign has been introduced to take care of the relative minus in eq.(93). The expression for $n_I(E)$ follows from (95),

$$e^{-2\pi i n_I(E)} = \lim_{N \rightarrow \infty} e^{-iE \log N} e^{-2i\alpha} \prod_{n=1}^N \frac{\varepsilon_n + iE/2}{\varepsilon_n - iE/2}. \quad (97)$$

Using the eqs.

$$\frac{1}{\Gamma(z)} = ze^{\gamma z} \prod_{n=1}^{\infty} \left(1 + \frac{z}{n}\right) e^{-z/n}, \quad (98)$$

$$\gamma = \lim_{N \rightarrow \infty} \left(\sum_{n=1}^N \frac{1}{n} - \log N \right), \quad (99)$$

one finds

$$\lim_{N \rightarrow \infty} e^{-iE \log N} \prod_{n=1}^N \frac{n+a+iE/2}{n+a-iE/2} = \frac{\Gamma(1+a-iE/2)}{\Gamma(1+a+iE/2)}, \quad (100)$$

which plugged in (97), and taking the log, gives

$$n_I(E) = \frac{1}{\pi} \log \Gamma \left(1 + a + i \frac{E}{2} \right) + \frac{\alpha}{\pi}. \quad (101)$$

Comparing this equation with the smooth part of the Riemann's counting formula (7), we deduce that the Gamma term in both eqs. agree if we choose

$$a = -\frac{3}{4}. \quad (102)$$

The energy levels ε_n (see eq. (94)) corresponding to this choice are those of a harmonic oscillator with zero point energy $1/4$, instead of $1/2$. This vacuum energy arises from Neumann BC's at the origin which select the even eigenfunctions under parity. In this sense the RD model can also be seen as a harmonic oscillator with Neumann BC's perturbed by the g_D and h_D interactions given in eq.(25).

The asymptotic expansion of (101) gives the finite part of (93), and it is related to the smooth part of the Riemann formula (7), for $\alpha = \pi/2$, as

$$N_{\text{sm}}(E) = n_I(E) - \frac{E}{2\pi} \log \pi + \frac{1}{2}. \quad (103)$$

Notice again the term $-E/2\pi \log \pi$ which, as we said, is regularization dependent. To highlight this point, we shall apply a zeta function regularization to the expression (97). Choosing $N = \infty$ one has formally,

$$e^{-2\pi i \hat{n}_I(E)} = e^{-2i\alpha} \frac{\prod_{n=1}^{\infty} \mu(\varepsilon_n + iE/2)}{\prod_{n=1}^{\infty} \mu(\varepsilon_n - iE/2)}, \quad (104)$$

where $-\widehat{n}_I(E)$ stands for the regularized value of $N_I(E)$ and μ is a regulator. The infinite products in (104) can be regularized using the zeta function [37]

$$\prod_{n=0}^{\infty} \mu(n+z) = \mu^{1/2-z} \left(\frac{1}{\sqrt{2\pi}} \Gamma(z) \right)^{-1}. \quad (105)$$

The result is

$$e^{-2\pi i \widehat{n}_I(E)} = e^{-2i\alpha} \mu^{-iE} \frac{\Gamma(1+a-iE/2)}{\Gamma(1+a+iE/2)}, \quad (106)$$

and

$$\widehat{n}_I(E) = \frac{1}{\pi} \log \Gamma \left(1 + a + i \frac{E}{2} \right) + \frac{\alpha}{\pi} + \frac{E}{2\pi} \log \mu. \quad (107)$$

Choosing $\mu = 1/\pi$ one gets the factor $-E/2\pi \log \pi$, and the relation (103) is replaced by

$$N_{\text{sm}}(E) = \widehat{n}_I(E) + \frac{1}{2}. \quad (108)$$

There is also a mismatch of $1/2$ due to the α term, which is not important for large values of E but which can be relevant for small ones. We have carried out a numerical computation to assess the accuracy of $N_{\text{sm}}(E_n)$ for predicting the position of the zeros (E_n is the imaginary part of the n^{th} Riemann zero). The closest $N_{\text{sm}}(E_n)$ comes to n , the better the approximation is. The results for the first 10 zeros are collected in table 1. They show that $N_{\text{sm}}(E) + 1/2 = \widehat{n}_I(E) + 1$ is a much better fit than $N_{\text{sm}}(E)$, suggesting that the zeros are associated to complete RG cycles. This result is confirmed in figure 6, where we plot the difference $n - N_{\text{sm}}(E_n) - 1/2$ for the first 40 zeros. This extra factor $1/2$, that improves the location of the zeros, was also obtained by Berry [6] and Badhuri et al. [30] in their respective approaches.

n	1	2	3	4	5	6	7	8	9	10
E_n	14.1347	21.0220	25.0109	30.4248	32.9350	37.5861	40.9187	43.3270	48.0051	49.7738
$N_{\text{sm}}(E_n)$	0.4497	1.5702	2.3936	3.6710	4.3172	5.5935	6.5651	7.2943	8.7708	9.3483
$N_{\text{sm}}(E_n) + \frac{1}{2}$	0.9497	2.0702	2.8936	4.1710	4.8172	6.0935	7.0651	7.7943	9.2708	9.8483

Table 1.- Values of the smooth part of the Riemann counting formula, $N_{\text{sm}}(E_n)$ for the first 10 Riemann zeros E_n (eq.(7)). $N_{\text{sm}}(E_n) + 1/2$ is also given for comparison.

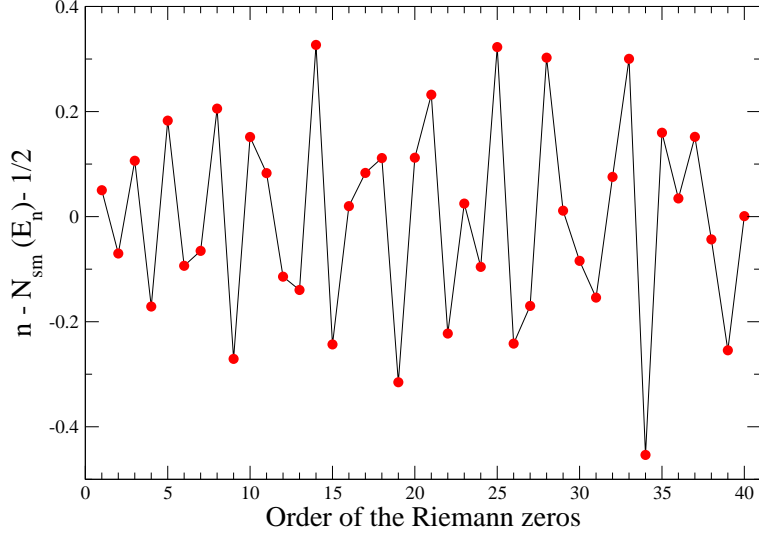


FIG. 6: Deviation of the first 40 zeros. The mean and square mean of $n - N_{\text{sm}} - 1/2$ are given by -0.003825 and 0.188102 respectively.

The oscillations in $n - N_{\text{sm}}(E_n) - 1/2$ are randomly distributed due to its relation to $\zeta(1/2 + iE)$. This fact implies that the uniform \mathcal{I} -model, eventhough describes the smooth part of the Riemann's zeros, does not explain the origin of their randomness.

To solve this problem we have tried to modify the uniform energy levels (94) in several ways. The first one is to modify the position of the energy levels. A slight modification of (94) consist in the addition of a $1/n$ correction,

$$\varepsilon_n = n + a + \frac{c}{n}, \quad n = 1, 2, \dots, N, \quad (109)$$

which does not change the $\log N$ behaviour of N_I . Using (97) one readily finds

$$n_I(E) = \frac{1}{\pi} \log [\Gamma(1 + a_+(E)) \Gamma(1 + a_-(E))] + \frac{\alpha}{\pi}, \quad (110)$$

where

$$a_{\pm}(E) = \frac{1}{2} \left[a + i\frac{E}{2} \pm \sqrt{\left(a + i\frac{E}{2} \right)^2 - 4c} \right]. \quad (111)$$

For large values of E , eq.(110) agrees with eq.(93) to order $E \log E$, but the comparison with (7) is lost since we have now the product of two gamma functions instead of one, as in (101). Adding higher order corrections to (109) of the form $1/n^2, \dots$ gives similar results.

Another possibility is to eliminate some energy levels in ε_n , for example those associated to the prime numbers. This choice is suggested by the quantum chaos hypothesis according to which the primitive orbits of the chaotic Hamiltonian are labelled by the primes [14, 15]. The truncation of the prime energy levels, i.e. ε_p (with p a prime), changes the asymptotic expansion of N_I which behaves as $\log(N/\log N)$ instead of $\log N$. However its finite part, n_I , does not improve the location of the Riemann zeros. These negative results can be understood from the formula (87) for N_I . Indeed, the function $\text{Arctan}(E/2\varepsilon_n)$ varies smoothly between 0 and $\pi/2$ in a range of E set by ε_n . The same applies for a superposition of those terms with different energies, making very difficult to obtain a random curve interpolating the zeros. The uniform energy levels seems to provide the best possible approximation within the \mathcal{I} model. This fact has lead us to a further generalization of this model.

VI. THE \mathcal{I}_\pm MODELS

The couplings $g_{I,D}$ have so far played an auxiliary role in the construction of the \mathcal{I} model. They appear in the renormalization and the exact solution, but they did not take part in the dynamics except for setting the boundary conditions. This suggests that $g_{I,D}$ must play a more significant role in the dynamics underlying the Riemann zeros. A natural generalization is to replace g_I , in the Hamiltonian (19), by a generic real symmetric matrix $g_{n,m}^I$, however the h_I interaction, no longer keeps its simple form under the RG, becoming a generic matrix. Surprisingly enough, there are two choices of $g_{n,m}^I$, which leave the h_I term invariant under the RG. The corresponding Hamiltonians are given by,

$$\langle n|H_{I_\pm}|m\rangle = \frac{1}{2}f_n (g_{I_\pm}(n, m) + ih_I \text{sign}(n - m)) f_m, \quad (112)$$

where the matrix elements $g_{I_\pm}(n, m)$ are defined in terms of a set of couplings $g_{I,p}$ ($p = 1, \dots, N$) as

$$g_{I_\pm}(n, m) = g_{I,p}, \quad p = \begin{cases} \max(n, m) & \text{for } \mathcal{I}_+ \\ \min(n, m) & \text{for } \mathcal{I}_- \end{cases}. \quad (113)$$

The structure of $g_{I_\pm}(n, m)$ is displayed in fig. 7, which also shows the direction in which the models are renormalized. For N finite the \mathcal{I}_\pm models are related by the transformation

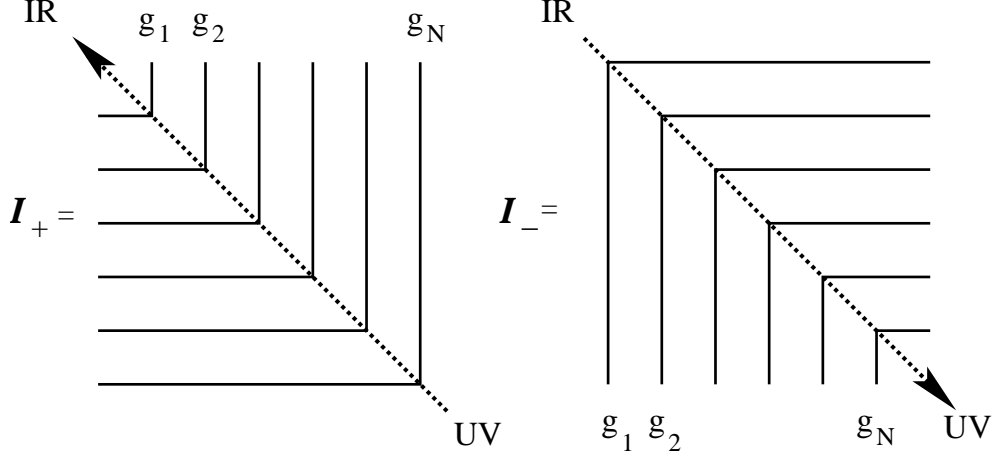


FIG. 7: Graphical representation of the coupling matrices $g_{I_{\pm}}(n, m)$ given in eq.(113). The continuous lines represent common values of $g_p = g_{I,p}$. The labels n, m (and the energies ε_n) increase from left to right and from top to bottom. The RG in the \mathcal{I}_+ model runs towards the infrared (IR) and in the \mathcal{I}_- model towards the ultraviolet (UV).

$n \rightarrow N - n$ and $h_I \rightarrow -h_I$, which changes the order of the energy levels ε_n . However in the limit $N \rightarrow \infty$ they are inequivalent. We shall assume, as usual, that ε_n increases with n .

The correspondence between eigenstates of the \mathcal{I} and the RD models is also maintained for \mathcal{I}_{\pm} , defining the associated RD_{\pm} models as

$$\langle n | H_{\text{RD}_{\pm}} | m \rangle = \varepsilon_n \delta_{n,m} - \frac{1}{2} (g_{D_{\pm}}(n, m) + i h_D \text{sign}(n - m)), \quad (114)$$

where $g_{D_{\pm}}(n, m)$ has the form (113), with $g_{I,p}$ replaced by $g_{D,p}$. The relation is established between an eigenstate, with energy E_I , of the \mathcal{I}_{\pm} models and the zero energy state, $E_{\text{RD}_{\pm}} = 0$ of the RD_{\pm} , with couplings constants given by eqs.(31), where the equation $g_D = g_I/E_I$ is replaced by $g_{D,p} = g_{I,p}/E_I$. If $g_{I,p} = g_I, \forall p$ the \mathcal{I}_{\pm} models reduce to the original \mathcal{I} model and the same applies to the RD_{\pm} models which become the RD one.

From a physical viewpoint the \mathcal{I}_+ and RD_+ models are characterized by the fact that the tunneling among two energy levels, induced by the g couplings, depends only on the state with the highest level n , i.e. the highest energy one for RD_+ . For the \mathcal{I}_- and RD_- models, it is the lowest level that matters. Looking at fig.4 one realizes that these models have to be renormalized in different ways for $h_{I,D}$ to be invariant. In the RD_+ model one has to eliminate the highest energy mode, $n = N$, which involves the product $(g_{D,N} + i h_D)(g_{D,N} - i h_D)$ which

is real, leaving h_D invariant. However, in the RD_- model, the level to be eliminated is $n = 1$, which also lives h_D fixed. Hence the RG flow goes towards the infrared in the RD_+ model, and towards the ultraviolet for RD_- . Of course the RD model can be renormalized in both ways. We shall not write explicitly the RG eqs. for the couplings but they can be easily derived using the techniques of section IV.

A. Continuum limit

Let's first consider the RD_+ model which, as we said, corresponds to \mathcal{I}_+ . The Schödinger eq.(114), for a state with $E_{RD} = 0$, is

$$\varepsilon_n \phi_n = \frac{1}{2} \sum_{m=1}^n g_{D,n} \phi_m + \sum_{m=n+1}^N g_{D,m} \phi_m + i h_D \sum_{m=1}^N \text{sign}(n-m) \phi_m, \quad (115)$$

and in the continuum

$$\varepsilon(n) \phi(n) = \frac{1}{2} \int_1^n dm g_D(n) \phi(m) + \frac{1}{2} \int_n^N dm g_D(m) \phi(m) + \frac{i h_D}{2} \int_1^N dm \text{sign}(n-m) \phi(m). \quad (116)$$

The derivative respect to n

$$\frac{d}{dn} [\varepsilon(n) \phi(n)] = i h_D \phi(n) + \frac{1}{2} \frac{dg_D}{dn} \int_1^n dm \phi(m), \quad (117)$$

is an integro-differential equation for $\phi(n)$, subject to the boundary condition

$$\varepsilon(N) \phi(N) = \frac{1}{2} (g_D(N) + i h_D) \int_1^N dm \phi(m). \quad (118)$$

Eq.(117) can be converted into a second order differential equation for the function

$$\chi(n) = \int_1^n dm \phi(m), \quad \phi(n) = \frac{d\chi}{dn}, \quad (119)$$

namely

$$\frac{d}{dn} \left(\varepsilon(n) \frac{d\chi}{dn} \right) - i h_D \frac{d\chi}{dn} - \frac{1}{2} \frac{dg_D}{dn} \chi = 0. \quad (120)$$

together with the BC's

$$\chi(1) = 0, \quad \varepsilon \frac{d\chi}{dn}(N) = \frac{1}{2}(g_D(N) + ih_D)\chi(N). \quad (121)$$

Making the change of variables $n \rightarrow q$ (recall eq.(50)), the eqs.(120) and (121) become

$$\frac{d^2\chi}{dq^2} - ih_D \frac{d\chi}{dq} - \frac{1}{2} \frac{dg_D}{dq} \chi = 0, \quad (122)$$

$$\chi = 0 \quad (\text{at } q = 0), \quad \frac{d\chi}{dq} = \frac{1}{2}(g_D + ih_D)\chi \quad (\text{at } q = L_N). \quad (123)$$

The second summand in eq.(122) can be eliminated by the gauge transformation,

$$\tilde{\chi} = e^{-ih_D q/2} \chi, \quad (124)$$

leading to

$$\frac{d^2\tilde{\chi}}{dq^2} - \frac{1}{2} \frac{dg_D}{dq} \tilde{\chi} + \frac{h_D^2}{4} \tilde{\chi} = 0, \quad (125)$$

$$\tilde{\chi} = 0 \quad (\text{at } q = 0), \quad \frac{d\tilde{\chi}}{dq} = \frac{1}{2}g_D \tilde{\chi} \quad (\text{at } q = L_N). \quad (126)$$

Notice that (125) is the Schrödinger equation of an *effective* Hamiltonian

$$H_+ = -\frac{d^2}{dq^2} + V_+(q), \quad V_+(q) = \frac{1}{2} \frac{dg_D}{dq}, \quad (127)$$

corresponding to a potential given by the derivative of the function $g_D(q)$. The energy of that state is given by $E_+ = h_D^2/4$. It is interesting to rederive the results obtained in previous sections where g_D is constant, i.e. $V_+ = 0$. The solution of eq.(125) gives a superposition of plane waves

$$\tilde{\chi} = e^{ih_D q/2} + C e^{-ih_D q/2}, \quad (128)$$

where $C = -1$ to satisfy the BC at $q = 0$ (eq.(126)). The BC at $q = L_N$ gives the plane wave quantization (see eqs.(40) and (51))

$$e^{ih_D L_N} = \frac{g_D + ih_D}{g_D - ih_D}. \quad (129)$$

The RD₋ model can be studied in a similar manner. We give for completeness the results. The function $\chi(n)$ must be defined as

$$\chi(n) = \int_n^N dm \phi(m), \quad \phi(n) = -\frac{d\chi}{dn}. \quad (130)$$

$\tilde{\chi}$ is still given by eq.(124). The effective Hamiltonian for $\tilde{\chi}$ is

$$H_- = -\frac{d^2}{dq^2} + V_-(q), \quad V_-(q) = -\frac{1}{2} \frac{dg_D}{dq}, \quad (131)$$

and the eigenenergies are given by the same formula $E_- = h^2/4$. The BC's also change

$$\frac{d\tilde{\chi}}{dq} = -\frac{1}{2}g_1 \tilde{\chi} \quad (\text{at } q = 0), \quad \tilde{\chi} = 0 \quad (\text{at } q = L_N). \quad (132)$$

As in the \mathcal{I} model these results can be generalized to the discrete case, obtaining an exact equation for the eigenvalues of the \mathcal{I}_\pm hamiltonians. The analogue of eq.(85) is a matrix like Bethe equation, related to the fact that the wave function $\tilde{\chi}_n$ satisfies a second order discrete differential equation. The results will be presented elsewhere.

Eqs. (122) and (131) bring the idea of a potential V_+ or V_- , whose scattering theory would produce the oscillating part of the Riemann counting formula. Pavlov and Fadeev showed long time ago that the zeta function $\zeta(s)$, on the line $Re(s) = 1$, appears in the scattering phase shift of particles moving on surfaces of constant negative curvature [38, 39, 40]. This is a possible direction of research, which is likely to be related to quantum chaos. On the other hand, our approach is based on discrete Hamiltonians, so the solution of the previous problem is a possible strategy to find the correct choice of the discrete couplings g_n leading to the precise location of the Riemann zeros.

On more general grounds, let us recall that one of the motivations to consider the Hamiltonian xp was the breaking of time reversal symmetry, which should be related to the GUE statistics of the zeros. This Hamiltonian gives an accurate semiclassical description of them but not of their fluctuations. The \mathcal{I}_\pm models break time reversal, but they also break the reversal of the RG time direction. Could this additional breaking be related to the GUE statistics of the zeros?

There are another interesting questions regarding the integrability of the models considered in this paper. The RD model, including its many body version, is exactly solvable à la Bethe and integrable (i.e. infinite number of conserved quantities) [34]. Thanks to the map

$\mathcal{I} \rightarrow \text{RD}$, we have been able to solve the \mathcal{I} model and in turn the regularized BK model. Is the \mathcal{I} model, including its many body version, integrable? It is not obvious how to generalize the map $\mathcal{I} \rightarrow \text{RD}$ to the many body case, due to the existence of several rapidity variables. The QM \mathcal{I}_{\pm} models are renormalizable and exactly solvable, although the analogue of the Bethe equation has a more complex structure. In the RD model the coupling g_D parameterizes a boundary operator in the transfer matrix of an inhomogenous vertex model. The existence of several couplings $g_{D,n}$ suggests that the corresponding transfer matrix, if it exists, involves more than one boundary operator.

VII. CONCLUSIONS AND PROSPECTS

We have shown in this paper that the Berry and Keating Hamiltonian can be quantized in a consistent way on a lattice. This quantization has been achieved thanks to the relation of the BK Hamiltonian to two QM models which have a cyclic RG, specially the RD model of superconductivity. The later models are renormalizable and have an exact solution à la Bethe, which permits a detailed study of their spectrum.

The first of these models, i.e. the \mathcal{I} model, is the inverse of the BK Hamiltonian plus an extra coupling which, in the BCS framework, is the standard pairing interaction. This model has a continuum spectrum related to RG cycles with an energy dependent period. The second model is the RD model, which has bound states related by a scale factor which depends on a fixed RG period. These two models are intimately related, since an eigenstate with energy E of the \mathcal{I} model, can be mapped into a bound state at the threshold of an RD model whose RG period is given by E . The map, which is exact, establish an unexpected correspondence between the BK model and the RD model of superconductivity where the time reversal symmetry is broken explicitly.

Using these QM models we have given an spectral interpretation of the smooth part of the Riemann counting formula of the non trivial zeros. In the \mathcal{I} model it counts the missing states in the continuum spectrum below a given energy. The result depends on the cutoff, which in our case is given by the number of sites. This result seems to agree with Connes's absorption spectral interpretation in the adelic theory, but the cutoff is different and a precise comparison with ours is not conclusive. In the RD model, the smooth part of the Riemann formula gives the number of missing bound states with respect to the leading term which

follows from the scaling properties of the cyclic RG. It is a finite size correction of the Russian doll scaling. In a certain sense, it can also be seen as an anomaly for the discrete RG transformations, i.e. the RG cycles, which leave the Hamiltonians invariant.

We have looked for a choice of parameters of the \mathcal{I} model that would explain the oscillating part of the Riemann formula. In the RD language this means choosing the energy levels. However a numerical study shows that the best choice is given by equally spaced energy levels. It thus seems that the origin of the random position of the zeros lies beyond the \mathcal{I} model. To explain this randomness we propose a natural generalization of the \mathcal{I} and RD models where the coupling g is replaced by a set of discrete couplings g_n which depend on the level n . The guiding principle is renormalizability, which in this context means the RG invariance of the time reversal breaking interaction. Quite surprisingly, there are two models, \mathcal{I}_\pm , satisfying this condition. They differ in the way the RG procedure is implemented. In the \mathcal{I}_+ model, the RG runs from the UV towards the IR, while in the \mathcal{I}_- model the order is reversed.

Finally, we have begun to explore the properties of the \mathcal{I}_\pm models in the continuum limit, finding two QM models with different potentials related to the gradient of the coupling function g_n and different boundary conditions. We suggest that an appropriate choice of these potentials, and in turn of the couplings constants g_n , may explain the local fluctuations of the Riemann zeros. The \mathcal{I}_\pm models are likely to be related to other approaches to the Riemann zeros, specially to quantum chaos. It would be interesting to investigate that connection.

Acknowledgments. I would like to thank A. LeClair for collaborating in the first stages of this work and for many clarifying discussions. I also thank M. Asorey, J. García-Esteve, M.A. Martín-Delgado, G. Mussardo, J. Rodríguez-Laguna and J.M. Román for conversations. This work is supported by the CICYT of Spain under the contract BFM2003-05316-C02-01. I also acknowledge the EC Commission for financial support via the FP5 Grant HPRN-CT-2002-00325 and the ESF Science Programme INSTANS 2005-2010.

[1] H.M. Edwards, “Riemann’s Zeta Function”, Academic Press, New York, 1974.

[2] See M. Watkins at <http://www.maths.ex.ac.uk/mwatkins> for a comprehensive review on several approaches to the RH.

- [3] H. Montgomery, “The pair correlation of zeros of the zeta function”, Analytic Number Theory, AMS (1973).
- [4] A. Odlyzko, “On the distribution of spacings between zeros of zeta functions”, Math. Comp. **48**, 273 (1987).
- [5] M. L. Mehta, “Random matrices”, Academic Press (1991).
- [6] M.V. Berry, in *Quantum Chaos and Statistical Nuclear Physics*. Eds. T.H. Seligman and H. Nishioka, Lecture Notes in Physics, No. 263, Springer Verlag, New York, 1986.
- [7] B. Julia, “Statistical theory of numbers”, in Number Theory and Physics, Springer Proceedings in Physics, **47** (1990).
- [8] J.-B. Bost and A. Connes, “Hecke algebras, Type III factors and phase transitions with spontaneous symmetry breaking in number theory”. *Selecta Mathematica, New Series* **1**, No. 3, 411, (1995).
- [9] M. Pitkänen, “Riemann hypothesis and superconformal invariance”, math.GM/0102031.
- [10] C. Castro, “On p-adic stochastic dynamics, supersymmetry and the Riemann conjecture” *Chaos Solitons & Fractals* **15**, 15 (2003); physics/0101104.
- [11] E. Elizalde, V. Moretti, S. Zerbini, “On recent strategies proposed for proving the Riemann hypothesis”, *Int.J.Mod.Phys.* **A18** (2003) 2189-2196; math-ph/0109006.
- [12] H.C. Rosu, “Quantum hamiltonians and prime numbers”, *Mod. Phys. Lett.* **A18** (2003) 1205; quant-ph/0304139.
- [13] G. Mussardo, “The Quantum Mechanical Potential for the Prime Numbers”, cond-mat/9712010.
- [14] M.V. Berry and J.P. Keating, “ $H=xp$ and the Riemann zeros”, in *Supersymmetry and Trace Formulae: Chaos and Disorder*, ed. J.P. Keating, D.E. Khmelnitskii and I. V. Lerner, Kluwer 1999.
- [15] Berry MV, Keating JP, “The Riemann zeros and eigenvalue asymptotics”, *SIAM REVIEW* **41** (2) 236, 1999.
- [16] K. G. Wilson, “Renormalization Group and Strong Interactions”, *Phys. Rev.* **D3** (1971) 1818.
- [17] P. F. Bedaque, H.-W. Hammer, and U. van Kolck, “Renormalization of the Three-Body System with Short-Range Interactions”, *Phys. Rev. Lett.* **82** (1999) 463, nucl-th/9809025.
- [18] D. Bernard and A. LeClair, “Strong-weak coupling duality in anisotropic current interactions”, *Phys.Lett.* **B512** (2001) 78; hep-th/0103096.

- [19] A. LeClair, J.M. Román and G. Sierra, “Russian doll Renormalization Group and Kosterlitz-Thouless Flows”, Nucl. Phys. **B675** (2003) 584; hep-th/0301042.
- [20] S. D. Glazek and K. G. Wilson, “Limit cycles in quantum theories”, Phys. Rev. Lett. **89** (2002) 230401, hep-th/0203088; “Universality, marginal operators, and limit cycles”, Phys. Rev. **B69**, 094304 (2004); cond-mat/0303297.
- [21] A. LeClair, J.M. Román and G. Sierra, “Russian doll Renormalization Group and Superconductivity”, Phys. Rev. **B69** (2004) 20505; cond-mat/0211338.
- [22] “The elementary excitations of the exactly solvable Russian doll BCS model of superconductivity”, A. Anfossi, A. LeClair, G. Sierra, J. Stat. Mech. (2005) P05011; cond-mat/0503014.
- [23] E. Braaten, H.-W. Hammer, and M. Kusunoki, “Efimov States in a Bose-Einstein Condensate near a Feshbach Resonance”, Phys.Rev.Lett. **90** (2003) 170402, cond-mat/0206232.
- [24] E. Braaten and H.-W. Hammer, “An Infrared Renormalization Group Limit Cycle in QCD”, Phys.Rev.Lett. **91** (2003) 102002, nucl-th/0303038.
- [25] A. LeClair, J.M. Román and G. Sierra, “Log-periodic behaviour of finite size effects in field theory models with cyclic renormalization group”, Nucl. Phys. **B700** [FS] (2004) 407; hep-th/0312141.
- [26] A. LeClair, and G. Sierra, “Renormalization group limit-cycles and field theories for elliptic S-matrices”, Theor. Exp. (2004) P08004; hep-th/0403178.
- [27] E. Braaten and H.-W. Hammer, “Universality in Few-body Systems with Large Scattering Length”, cond-mat/0410417.
- [28] I.R. Klebanov and M. J. Strassler, “Supergravity and a Confining Gauge Theory: Duality Cascades and χ SB-Resolution of Naked Singularities”, JHEP 0008 (2000) 052, hep-th/0007191.
- [29] A. Morozov and A. J. Niemi, “Can Renormalization Group Flow End in a Big Mess?”, Nucl. Phys. **B666**, 311 (2003); hep-th/0304178.
- [30] R.K. Bhaduri, A. Khare, and J. Law, “The phase of the Riemann function and the inverted harmonic oscillator”, Phys. Rev. **E52**, 486 (1995), chao-dyn/9406006; R.K. Bhaduri, A. Khare, S.M. Reimann, and E.L. Tomusiak, “The Riemann Zeta function and the inverted harmonic oscillator”, Ann. Phys. 254, 25 (1997).
- [31] A. Connes, “Trace formula in noncommutative geometry and the zeros of the Riemann zeta function”, Selecta Mathematica (New Series) 5 (1999) 29; math.NT/9811068.
- [32] J. Bardeen, L.N. Cooper and J.R. Schrieffer, “Theory of Superconductivity”, Phys. Rev. **108**,

- 1175 (1957).
- [33] J.R. Schrieffer, “Theory of Superconductivity”, *Frontiers in Physics*, Addison-Wesley Pub., New York (1988).
 - [34] C. Dunning and J. Links, “Integrability of the Russian doll BCS model”, *Nucl. Phys.* **B702** (2004) 481, cond-mat/0406234.
 - [35] J. von Delft and D. C. Ralph, “Spectroscopy of discrete energy levels in ultrasmall metallic grains”, *Physics Reports*, **345**, 61 (2001), cond-mat/0101019.
 - [36] J. Dukelsky, S. Pittel and G. Sierra, “Exactly solvable Richardson-Gaudin models for many-body quantum systems”, *Rev. Mod. Phys.* 76 (2004) 643; nucl-th/0405011.
 - [37] C. Deninger, “Arithmetic Geometry and Analysis on Foliated Spaces”, math.NT/0505354
 - [38] B.S. Pavlov and L.D. Fadeev, “Scattering theory and automorphic functions”, *Sov. Math.* 3, 522 (1975), Plenum Publishing Corp. translation, N.Y;
 - [39] Lax and R.S. Phillips, *Scattering Theory for Automorphic Functions*, Princeton University Press, Princeton, 1976.
 - [40] M.C. Gutzwiller, “Stochastic behaviour in Quantum Scattering”, *Physica* **D7**, 341 (1983).